

# Features of ball impact in straight, curve and knuckle kicks in soccer

Kaoru Kimachi<sup>1</sup> , Masaaki Koido<sup>2</sup>, Sungchan Hong<sup>2</sup> ,  
Shuji Shimonagata<sup>3</sup>, Masao Nakayama<sup>2</sup> and Takeshi Asai<sup>2</sup>

Proc IMechE Part P:  
*J Sports Engineering and Technology*  
1–10

© IMechE 2022

Article reuse guidelines:

sagepub.com/journals-permissions

DOI: 10.1177/17543371221101234

journals.sagepub.com/home/pip



## Abstract

The quantitative relationship between kicking motion and ball behaviour can be easily explained by detecting the impact point and foot posture. In previous studies, the impact point of a kicking foot was difficult to capture using visual tracking. Thus, a virtual surface modelling technique was applied in this study to clarify the differences in the three-dimensional foot speed, impact point and foot posture between straight, curve, and knuckle kicks in soccer, as well as the relationship between the kick motion and ball rotation. An optical three-dimensional motion capture system (VICON) was used to record the kicking motion. The impact points of the straight, curve, and knuckle kicks were found to be centrally located in the instep area, at a lower (more downwards) inside area, and at the medial area between the instep and inside areas of the kicking foot, respectively. Moreover, an impact with a greater 'swing vector deviation angle (relative to the direction from the impact point to the centre of gravity of the ball)' is necessary for ball rotation. The impact point detection method employed in this study can be applied to other ball impact estimations beyond soccer kicks.

## Keywords

Soccer, impact point, foot posture, swing vector deviation angle, straight kick, curve kick, knuckle kick, football, ball speed

Date received: 19 November 2020; accepted: 20 April 2022

## Introduction

The kicking skills required to control ball rotation and trajectory are important in soccer. Studies on straight kicks to achieve higher ball speeds<sup>1–4</sup> and curve kicks for curving the ball trajectory using ball rotation<sup>5–9</sup> have been conducted. In addition, knuckle kicks, which can increase the possibility of scoring because they create an unstable trajectory that is difficult for the goalkeeper to react to, have recently become the subject of investigation.<sup>9–17</sup> Straight kicks with greater ball speeds can increase the possibility of scoring a goal by shortening the time available for goalkeepers to react. Straight kicks require considerably high ball speeds, frequently with back spin. Curve kicks rely on sideways ball rotation to generate curved trajectories that can take the ball away from the goalkeeper's reach. Knuckle kicks are characterised by their unstable trajectories.<sup>11</sup> Asai et al. reported that the unstable trajectory of a knuckle kick is caused by the floating (knuckling) effect induced by small ball rotation.<sup>7</sup> To determine the technical features of a knuckle kick performed with low rotation, it is necessary to clarify the impact point and its contribution to ball rotation.

The technical factors that affect ball-kicking include the 'foot speed', 'foot-to-ball speed ratio' and 'effective foot mass'.<sup>18,19</sup> The impact point is an important variable related to the foot-to-ball speed ratio, coefficient of restitution, and effective foot mass because some mechanical factors (moment arm from foot joint, rigidity of the point, etc.) will be changed based on the location of the impact point.<sup>1,3,20</sup> The angle of attack (attacking angle) correlates with the production of rotational forces.<sup>12</sup> The attacking angle can be determined by the foot posture at the moment when a ball impact occurs. Research literature reporting the effects of foot posture in kicking motions is currently scarce.

<sup>1</sup>Doctoral Program in Coaching Science, University of Tsukuba, Tsukuba, Japan

<sup>2</sup>Faculty of Health and Sports Sciences, University of Tsukuba, Tsukuba, Japan

<sup>3</sup>Faculty of Education, Chiba University, Chiba, Japan

### Corresponding author:

Kaoru Kimachi, Doctoral Program in Coaching Science, University of Tsukuba, 1-1-1, Tennodai, Tsukuba 3058577, Japan.

Email: human\_declined@yahoo.co.jp

The impact point is an index that indicates the starting point of the interaction of the forces acting between the foot and the ball. Detecting the three-dimensional impact point is an important step in explaining the quantitative relationship between the kicking motion and ball behaviour, not only in terms of ball speed, but also ball rotation. Ishii et al. calculated the distance between the centres of gravity of the foot and ball impact to determine the impact point in only the sagittal plane; the closer the impact point was to the centre of gravity of the foot, the greater the resulting ball speed.<sup>3</sup> Peacock and Ball represented the impact point as a two-dimensional coordinate (medial-lateral and proximal-distal) on a curved plane set on the surface of the instep area of a mechanical foot.<sup>4</sup> In that study, a sweet spot was found at which an impact produced the greatest ball speed. The foot-to-ball speed ratio, coefficient of restitution and effective foot mass were used to indicate the relationship between the ball behaviour (mainly represented by the ball speed) and the impact point. There have been some reports on impact points in projected coordinate values (two-dimension) and calculated distance (one-dimension), but not the three-dimensional detection of the impact point in ball kicking. A few optical high-speed measurements (2000 Hz) of impact points in kicking motions have been reported.<sup>21</sup> Kimachi et al. mentioned that a surface model composed of virtual markers enabled the detection of three-dimensional impact points.<sup>21</sup> This virtual modelling technique calculated the impact points by generating a rigid-body virtual surface for each segment until just prior to impact, rather than directly and visually estimating it as in previous studies. This approach enabled the impact surface detection of the foot and the ball to be observed in three-dimension in invisible space. Detailed analysis of the ball impact process could serve as a useful resource for players seeking to improve their kicking motion.

The present study clarified the features of ball impact and foot posture in straight, curve, and knuckle kicks by identifying impact points using an optical three-dimensional motion capture system and a virtual modelling technique. The differences between the three types of kicks on impact-point trajectory and ball rotation in the ball impact process were investigated. It was hypothesised that the differences in impact points and ball rotation according to kick types are quantified as three-dimensional coordinate value.

## Methods

### Participants

The participants in this study were 15 right-footed male collegiate soccer players with height:  $1.70 \pm 0.06$  m; body mass:  $65.6 \pm 5.1$  kg; and soccer experience:  $14.3 \pm 1.8$  years. The study design was approved by the appropriate ethics review board (P.E. 28-23: committee of the University of Tsukuba), and all participants

provided informed consent. The participants wore the same type of indoor shoes (Umbro) of suitable sizes. They performed three types of kicks (straight, curve and knuckle) five times each at maximum effort to obtain high ball speeds and the required ball rotation. One best trial in the five attempted shots was identified verbally by the participants to choose a successful trial for analysis. The VICON (2000 Hz: Oxford Metrics Ltd., Oxford, England) optical motion capture system with ten cameras was used in the experiment (Figure 1(a)). The global coordinate system was established in terms of the lateral ( $X$ -axis: right (+), left (-)), horizontal ( $Y$ -axis: forward (+), backward (-)), and vertical ( $Z$ -axis: upward (+), downward (-)) directions from the origin, which was set on the floor (Figure 1(a)). In this coordinate system, the horizontal plane and sagittal plane were the  $X$ - $Y$  planes and  $Y$ - $Z$  planes, respectively. A total of 41 reflective 15 mm spherical markers were placed on across the entire kicker body according to the preinstalled plug-in gait model in the NEXUS analysis software (Oxford Metrics Ltd., Oxford, England). The first and fifth metatarsal head markers were placed on the kicking foot together with a heel marker in the plug-in gait model to compose the foot segment. The centre of gravity of the foot (CGF) was set at the midpoint within the heel and metatarsal head markers, based on the definition of the plug-in gait model. Four reflective markers were also placed on the top, front, right, and left of the intersection points between the ball surface and the three axes originating from the centre of gravity of the ball (CGB) to compose the ball segment.

### Impact point detection

The impact points were detected using the NEXUS (Oxford Metrics Ltd., Oxford, England) analysis software. The impact point in this study was defined as the initial contact location between the foot (POF) and ball (POB). The impact surface, which could not be visually captured easily, was determined by a group of virtual markers that have coordinate values in the analysis software. That virtual impact surface denoted by the virtual markers was constructed using the captured real markers placed in a regular grid pattern on the real model shoe (Umbro) and the ball. The surface model was then created by spreading virtual markers between the captured real markers on the surface of the model shoe (Figure 1(d)) and the ball. These virtual markers represented the surface of the shoe and the ball as coordinate values in the local coordinate systems of the foot and ball segments,<sup>21</sup> and the group of virtual markers was called the virtual model in this study.

The foot segment was set on the right kicking foot using the following axes: the horizontal ( $Y_f$ ) direction from the heel (origin) to the midpoint of the metatarsal heads, the vertical ( $Z_f$ ) direction orthogonal to the plane composed of the three-foot segment markers, and the lateral ( $X_f$ ) direction orthogonal to the  $y$  and  $z$  axes

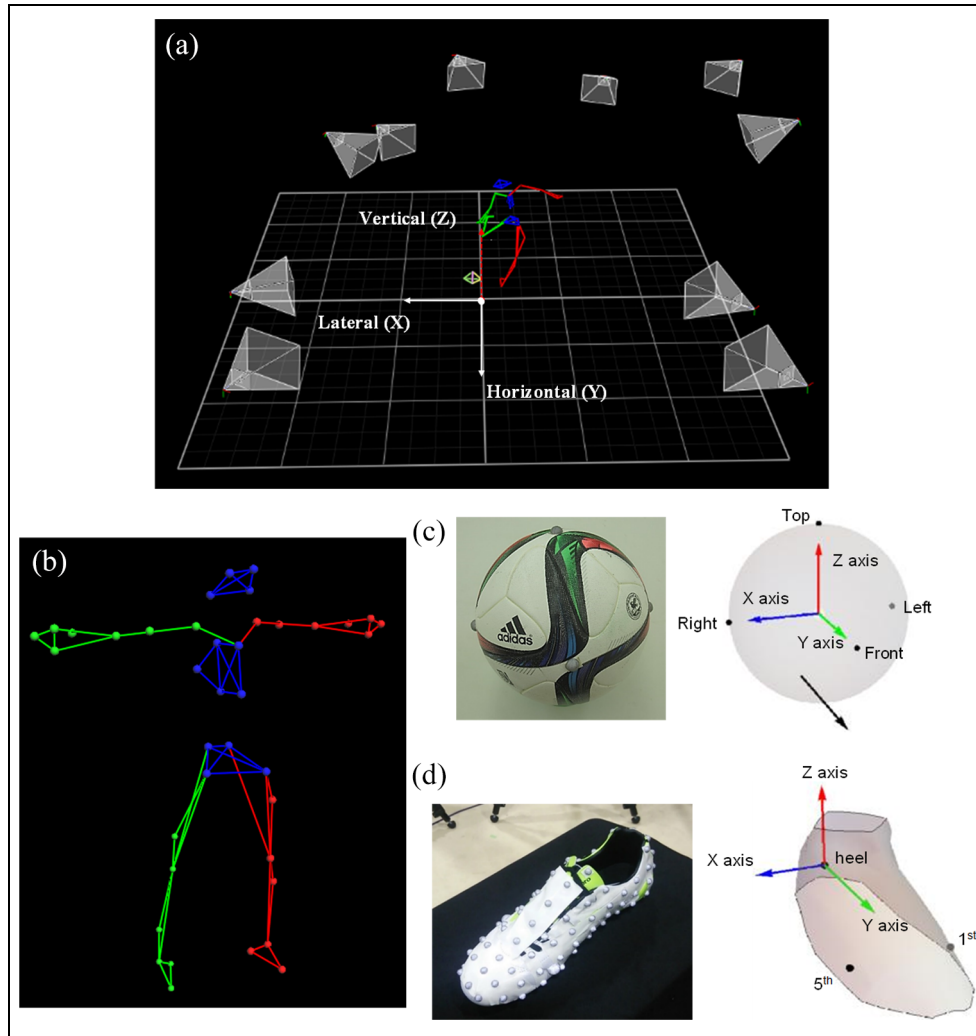


**Figure 1.** (a) Illustration of the global coordinate system used in this study with lined detector reflective markers of ball and whole body of participant. (b) 39 markers of whole body in the plug-in gait model. (c) Four markers on the ball and the local coordinate system on the ball segment. (d) Markers on the shoe to make foot segment and virtual surface of the virtual foot model and the local coordinate system.

in the direction of the fifth metatarsal head. The coordinate values of the virtual markers describing the foot segment were saved to apply to the captured motion. The size of the real shoe used for modelling was 265 mm. Therefore, virtual foot models of each trial constructed for each participant were stretched along the y-axis because the length ( $Y_f$ ) showed approximately twice the value of the standard deviation of the breadth ( $X_f$ ) and height ( $Z_f$ ) in Japanese foot measurement<sup>22</sup> to fit the size of the foot of each participant.

The origin of the local coordinate system of the ball was placed at the midpoint of the left and right markers (the centre of gravity of the ball). The axes were set as the horizontal ( $Y_b$ ) direction from the origin to the front marker; vertical ( $Z_b$ ) direction orthogonal to the plane composed by the front, left, and right markers; and lateral ( $X_b$ ) direction orthogonal and right to the  $Y_b$ -axis and  $Z_b$ -axis. The coordinate values of the virtual markers of the virtual ball model were calculated from the fixed value of the ball radius.

Virtual ‘rigid’ surface models displayed on the analysis software showed the timing of the impact by their collision. In each foot and ball virtual model, the paired markers showing the minimum distance at the impact timing were recorded as the impact points of each segment. Coordinate values were recorded in millimetres on each axis.

#### Data collection and statistical analysis

The mean speed of the CGB was recorded 0.005 s after the ball left the kicking foot as the ball speed. The mean speed of the POF was recorded 0.005 s before the ball impact as the foot speed. Foot-to-ball speed ratio was measured from the foot (POF) speed and ball speed. The extrapolation method was not used to avoid the loss of the peak value in the trend, though the extrapolated data differed from the mean speed by only 0.1 m/s on average. Ball rotation was calculated as sideways rotation (AVA = around vertical axis, counter-clockwise (+), clockwise (-)) and vertical rotation

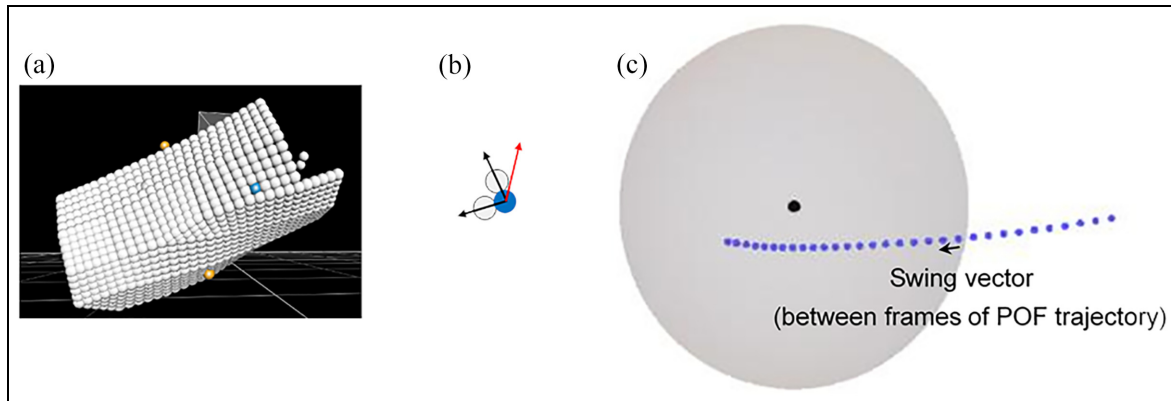


**Figure 2.** (a) Detected impact point of foot in the virtual model. (b) The face vector as a normal unit vector (red) was calculated as the cross-product vector of two vectors (black) from the POF (impact point on foot) to adjacent markers. (c) The swing vector was displacement between coordinate values of POF trajectory.

(ALA = around lateral axis, back (+), top (-)) of the ball segment in the global coordinate system in revolutions per second (rps). The distance from the CGF to the POF was calculated. The foot posture at the impact moment was recorded as a set of Euler angles (roll, pitch, and yaw). The ball deformation was estimated from contact time and minimum distance between POF and CGB during the impact. The POF trajectory (displacement of POF during the impact) was represented in three-dimensional coordinates (XYZ global coordinate system) with the origin slide to the initial CGB starting from 0.005 s before impact to 0.01 s after impact (almost when the foot and ball parted) and visualised on each plane. The face vector was constructed by calculating the cross product of vectors from the POF to the adjacent markers (Figure 2(b)) and represented as the angle from the resulting axis to the horizontal and vertical planes in each frame. The swing vectors were defined as displacement between each frame of the POF trajectory (Figure 2(c)). Both the face and swing vectors during ball impact were shown as mean angles on the horizontal and sagittal planes. In addition, the attacking angle between the face and swing vectors was calculated as angle differences on the horizontal and sagittal planes. The swing vector deviation angle was calculated as the deviation angle of the swing vector relative to the direction from the POF to the CGB during ball impact, and the correlation with ball rotation was examined.

The data for all participants were reported as mean  $\pm$  standard deviation. A paired *t*-test and Cohen's effect size (*d*)<sup>23,24</sup> were calculated to compare the various kick types. The level of significance was set at 0.05 in a three-group, one-way analysis of variance and modified by Bonferroni correction ( $0.05/3 = 0.017$ ) in each pair.

## Results and discussion

The results of this study are presented in Table 1 and discussed in detail in this section.

### Ball speed and rotation with validation

The ball speed, foot speed and ball rotations for the straight, curve, and knuckle kicks are shown in Table 1. No significant differences in the ball speed were observed. The foot speed of the knuckle kick was significantly smaller than that of the straight kick ( $p < 0.017$ ,  $d = 1.25$ ). There was no significant difference between the ball rotations of the straight and knuckle kicks in terms of AVA, but all other possible pairs showed significant differences.

The ball speed of the straight kick was the greatest for all kick types in this study; however, it was in the intermediate of the values reported in previous studies at 21.9 and 32.1 m/s.<sup>23</sup> The curve kick showed a greater ball rotation around the vertical axis. Asai et al. reported that the ball rotation of curve kicks ranged from 3.0 rps to more than 10.0 rps, depending on factors such as impact location and ball speed, which showed a maximum value of 26.0 m/s.<sup>5</sup> The ball rotation around the lateral axis of the knuckle kick was significantly smaller than that of the straight kick. A previous report showed unpredictable trajectories with ball rotation values of 20–40 rpm (0.33–0.67 rps) at ball speed greater than 15.0 m/s.<sup>25</sup> The results of every type of kick obtained in this study can thus be considered comparable to those obtained in previous studies.

### Point on ball, foot posture and point on foot

The POB of the straight, curve, and knuckle kicks are provided in Table 1 and shown in Figure 3. The straight kick had significantly smaller horizontal ( $p < 0.017$ ; vs. curve ( $d = 1.32$ ), knuckle ( $d = 1.67$ )) and larger vertical ( $p < 0.017$ ; vs. curve ( $d = 1.36$ ), knuckle ( $d = 1.43$ )) POB values than the other kick types. The curve kick had a significantly smaller lateral POB value than the knuckle kick ( $p < 0.017$ ; vs. straight ( $d = 0.94$ ), knuckle ( $d = 1.15$ )).

**Table 1.** Summary of variables and resultant foot posture and kick motion (mean  $\pm$  standard deviation) with notation of significance and *d*-effect size for three types of kicks (Straight (d: versus Curve), Curve (d: versus Knuckle), Knuckle (d: versus Straight)).

	Straight	Curve	Knuckle
Ball speed [m/s]	25.8 $\pm$ 1.5	24.9 $\pm$ 1.0	24.8 $\pm$ 1.9
<i>d</i>	0.69	0.08	0.57
Foot speed [m/s]	19.6 $\pm$ 0.7 ‡	19.1 $\pm$ 0.8	18.2 $\pm$ 1.6 ‡
<i>d</i>	0.55	0.92	1.25
Foot-to-ball speed ratio	1.32 $\pm$ 0.1 ‡	1.31 $\pm$ 0.1 †	1.38 $\pm$ 0.1 ††
<i>d</i>	0.33	1.37	0.95
Ball Rotation [rps]			
AVA	-0.3 $\pm$ 1.0*	5.2 $\pm$ 1.0*†	-0.04 $\pm$ 0.7†
ALA	2.1 $\pm$ 0.7*‡	-1.8 $\pm$ 1.4*†	0.7 $\pm$ 1.2††
<i>d</i>	5.58	5.90	0.29
	3.56	1.87	1.44
Impact point on ball [mm]			
Lateral	1.5 $\pm$ 4.9	-3.8 $\pm$ 6.4†	5.9 $\pm$ 10.1†
Horizontal	-107.7 $\pm$ 1.1*‡	-105.3 $\pm$ 2.3*	-105.1 $\pm$ 1.8†
Vertical	-20.0 $\pm$ 6.6*‡	-29.4 $\pm$ 7.2 *†	-28.9 $\pm$ 5.9 ††
<i>d</i>	0.94	1.15	0.56
	1.32	0.08	1.67
	1.36	0.07	1.43
Euler angle [degree]			
Roll	-37.8 $\pm$ 4.9*‡	-26.9 $\pm$ 6.0*	-30.7 $\pm$ 9.2‡
Pitch	-36.0 $\pm$ 7.4*‡	-5.1 $\pm$ 6.2*†	-20.0 $\pm$ 12.6††
Yaw	-35.9 $\pm$ 10.4*‡	-71.0 $\pm$ 8.4*†	-55.9 $\pm$ 14.4††
<i>d</i>	1.99	0.48	0.97
	4.51	1.49	1.55
	3.71	1.29	1.58
Impact point on foot [mm]			
Lateral	-26.8 $\pm$ 4.6 *‡	-37.1 $\pm$ 2.2 *	-35.3 $\pm$ 6.7 ‡
Horizontal	155.0 $\pm$ 5.1‡	151.3 $\pm$ 13.0†	143.3 $\pm$ 11.0††
Vertical	50.6 $\pm$ 1.7*	46.8 $\pm$ 3.9*†	50.0 $\pm$ 2.5†
<i>d</i>	2.84	0.37	1.47
	0.37	0.66	1.36
	1.26	0.96	0.29
Euler angle displacement [degree]			
Roll	5.4 $\pm$ 3.6*‡	13.2 $\pm$ 4.4*	11.6 $\pm$ 3.7‡
Pitch	8.5 $\pm$ 3.8	9.4 $\pm$ 2.4	8.4 $\pm$ 4.6
Yaw	-7.7 $\pm$ 4.5	-5.2 $\pm$ 4.2	-7.0 $\pm$ 5.7
<i>d</i>	1.95	0.41	1.70
	0.28	0.25	0.01
	0.59	0.36	0.15
Distance from POF to CGF [mm]	86.4 $\pm$ 2.4	85.9 $\pm$ 7.5	81.6 $\pm$ 4.5
<i>d</i>	0.08	0.69	1.31
Face vector angle [degree]			
Horizontal	-2.2 $\pm$ 4.4	-0.9 $\pm$ 6.6	-4.8 $\pm$ 10.0
Sagittal	10.7 $\pm$ 6.3*	24.4 $\pm$ 5.9*†	12.9 $\pm$ 13.7†
<i>d</i>	0.22	0.46	0.34
	2.25	1.10	0.20
Swing vector angle [degree]			
Horizontal	-0.3 $\pm$ 2.4*	21.3 $\pm$ 3.6*†	2.0 $\pm$ 3.0†
Sagittal	0.0 $\pm$ 2.5*‡	16.0 $\pm$ 5.6*†	5.5 $\pm$ 3.1††
<i>d</i>	7.07	5.84	0.84
	3.65	2.31	1.92
Attacking angle [degree]			
Horizontal	1.8 $\pm$ 4.1*	22.3 $\pm$ 7.0*†	6.8 $\pm$ 10.4†
Sagittal	-10.6 $\pm$ 5.7	-8.5 $\pm$ 7.7	-7.4 $\pm$ 14.9
<i>d</i>	3.56	1.75	0.62
	0.32	0.09	0.29

Significant differences ( $p < 0.017$ ) between pairs are indicated as follows; straight vs. curve (\*), curve vs. knuckle (†), straight vs. knuckle (‡). AVA means revolution around vertical axis, and ALA means revolution around lateral axis.

The Euler angles at the impact moment, which describe the foot posture in terms of the displacement angle components 0.01 s after the impact of the straight

kick, are also given in Table 1. Significant differences can be observed between all pairs of angle components, except between the roll components of the curve and

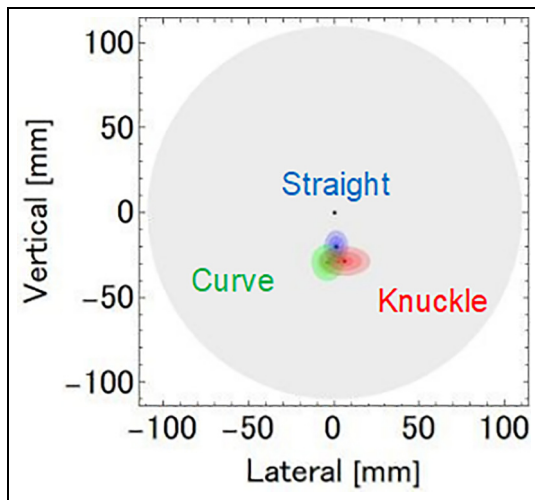


**Figure 3.** POB (impact point on ball) location of the straight (blue), curve (green), and knuckle (red) kicks on the frontal plane expressed by ellipses scaled to 1.5 times the standard deviation of the lateral and vertical axes.

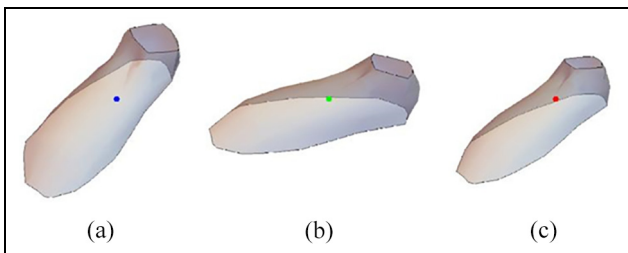


**Figure 4.** Foot posture for straight (a), curve (b), and knuckle (c) kicks.

knuckle kicks. It appears to indicate the similarity of the curve and the knuckle kick. Significant differences in displacement were found in the roll components of the straight versus curve and knuckle kicks. Foot posture images before and after the impact and transition of the Euler angles for the three kick types are shown in Figures 4 and 5.

The foot posture of the straight kick at impact resulted in a kick with an impact point similar to that identified by Peacock et al.<sup>20</sup> as the ‘sweet spot’ to produce the best result. The minimal inhibition of the front swing of the leg caused by the small roll angle led to an increase in foot speed. The foot posture of the curve kick at impact showed a slightly smaller negative pitch value than the other kicks and the greatest negative yaw value of all kicks. Impact with a horizontal surface, such as the inside of the kicking foot, can cause sideways ball rotation because of the increase in the face vector that may widen the attacking angle. The knuckle kick showed smaller negative pitch and roll values than the straight kick. These smaller values are among the ways of creating an impact closer to the

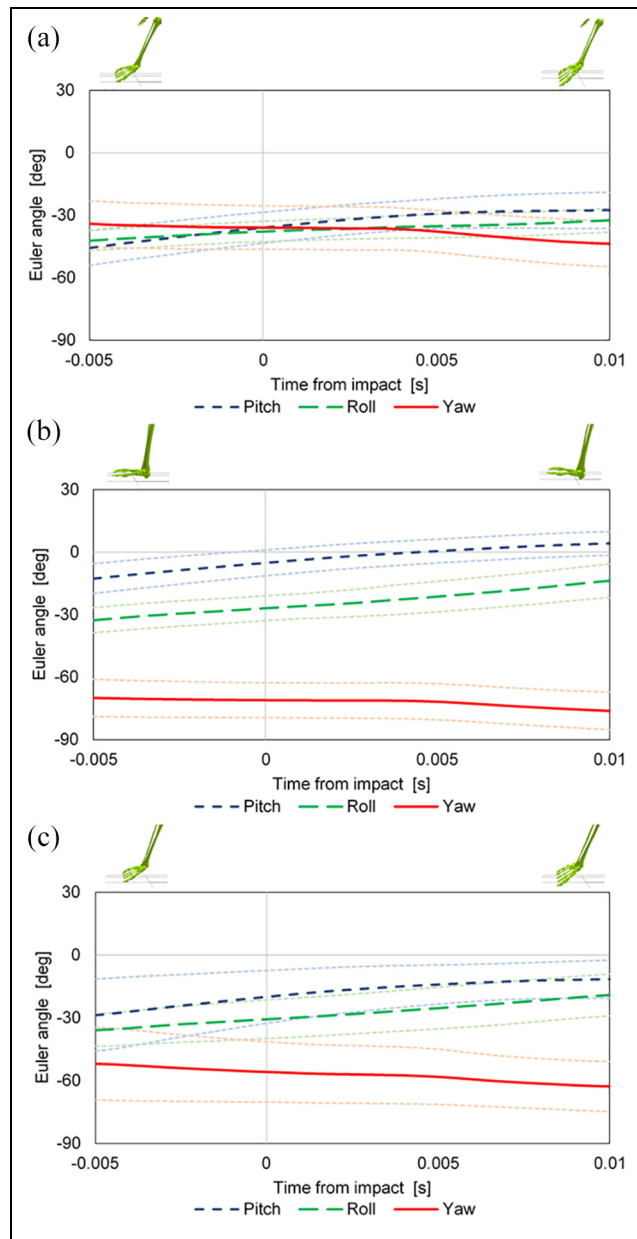


**Figure 5.** Transitions of the Euler angles (pitch is given by the short-dashed blue line, roll by the long-dashed green line, and yaw by the solid red line) from 0.005 s before the impact to 0.01 s after the impact for straight (a), curve (b), and knuckle (c) kicks with pictures of bones as foot posture of start and end timing viewed from the front.

CGF to decrease ball rotation and can be attributed to the posture of the foot at the impact moment of a knuckle kick, which was opened to the right, in contrast to a straight kick. The sagittal face vector angle value order of the three types of kicks indicated the order of ball rotation around the lateral axis.

The POE values of the straight, curve, and knuckle kicks are given in Table 1 and shown in Figure 6. The lateral POE of the straight kick was significantly larger than that of the other kick types ( $p < 0.017$ ; vs. curve ( $d = 2.84$ ), knuckle ( $d = 1.47$ )). The vertical POE of



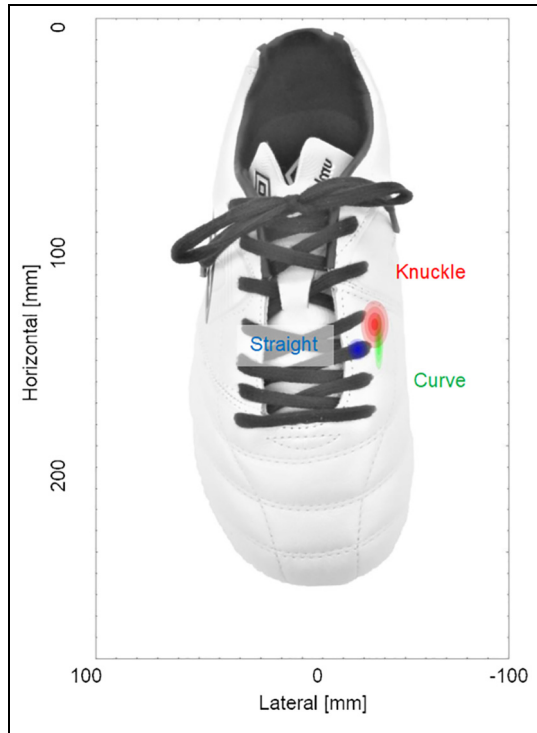


**Figure 6.** POF (impact point on foot) location of straight, curve, and knuckle kicks on the horizontal plane, expressed by ellipses scaled to 1.5 times the standard deviation along the lateral and horizontal axes.

the curve kick was significantly smaller than those of the other kick types ( $p < 0.017$ ; vs. straight ( $d = 1.26$ ), knuckle ( $d = 0.96$ )), and the horizontal POF of the knuckle kick was significantly smaller than those of the other kick types ( $p < 0.017$ ; vs. straight ( $d = 1.36$ ), curve ( $d = 0.66$ )). The distances from the CGF to the POF for the straight, curved, and knuckle kicks are provided in Table 1 as well, and the POF trajectories are shown in Figure 7.

The POF of all kick types was concentrated in a relatively rigid area (Figure 6) close to the medial cuneiform.<sup>1,3,20</sup> The POF of the knuckle kick was closer to the CGF than that of the curve kick to decrease ball rotation (regardless of differences in foot thickness). Based on this observation, it was found that knuckle kicks decrease ball rotation with a closer impact point to the CGF.

### Foot behaviour during ball impact

The ball deformation estimated from contact time (approximately 21 frame, 10.5 ms) and minimum distance (approximately 35.2 mm) between POF and CGB during the impact was not different between types of kicks.

The mean face and sagittal vector angles during the ball impact of the straight, curve, and knuckle kicks are given in Table 1. The mean sagittal face vector angle of the curve kick was significantly larger than

those of the other kick types ( $p < 0.017$ ; vs. straight ( $d = 2.25$ ), knuckle ( $d = 1.10$ )). The mean sagittal swing vector angle of the knuckle kick was significantly larger than that of the straight kick ( $p < 0.017$ ,  $d = 1.92$ ) but was smaller than that of the curve kick ( $p < 0.017$ ,  $d = 2.31$ ).

The mean values of the attacking angle transition during the ball impact of the straight, curve, and knuckle kicks are also shown in Table 1. A significant difference was only observed between the curve kick and the others in the horizontal direction ( $p < 0.017$ ; vs straight ( $d = 3.56$ ), knuckle ( $d = 1.75$ )).

On the horizontal plane, the POF trajectories of both the straight and knuckle kicks appear to be linear (Figure 7(g) and (i)). However, the POF trajectory of the knuckle kick, which has a lower POB, showed a greater sagittal swing vector angle and a greater sagittal face vector angle than that of the straight kick. On the horizontal plane, curve kicks showed significantly wider attacking angles than the other kick types. This result supports those of Hong et al., who compared straight, curve, and knuckle kicks.<sup>12</sup>

The transition of the swing vector deviation angle during ball impact is shown in Figure 8. The correlation coefficient between the mean swing vector deviation angle and the ball rotation was horizontal = 0.93 and sagittal = 0.83, as shown in Figure 9. From those high correlation coefficients between the mean swing vector deviation angle and ball rotation (Figure 9), the foot swing direction against the CGB can make the ball rotate in each plane during ball impact.

Capturing the three-dimensional location of the impact point and foot posture enabled the calculation of the swing and face vectors at every impact. This in turn enabled the verification of the correlation between kicking motion and ball rotation during ball impact.

By calculating the impact point and foot posture, it was deduced that the straight kick is conducted by striking the ball with the instep area of the foot, where a larger pitch angle (plantar flexion) and smaller foot trajectory can cause backside ball rotation. The curve kick is executed by striking the ball with the inside area of the foot, where a greater negative yaw angle can cause a sideways ball rotation. Finally, the knuckle kick is executed by striking the ball with the medial area of the foot between the instep and inside areas with a foot posture that faces the CGB. A foot trajectory that passes through an area close to the CGB can decrease ball rotation in the knuckle kick.

### Limitations and implications

In this study, the impact point was measured using a virtual foot model and significant differences in impact point coordinates were observed according to kick type. Note that the proposed method has a risk of coordinate value error of less than 2.9 mm because the maximum distance between the virtual markers used in the

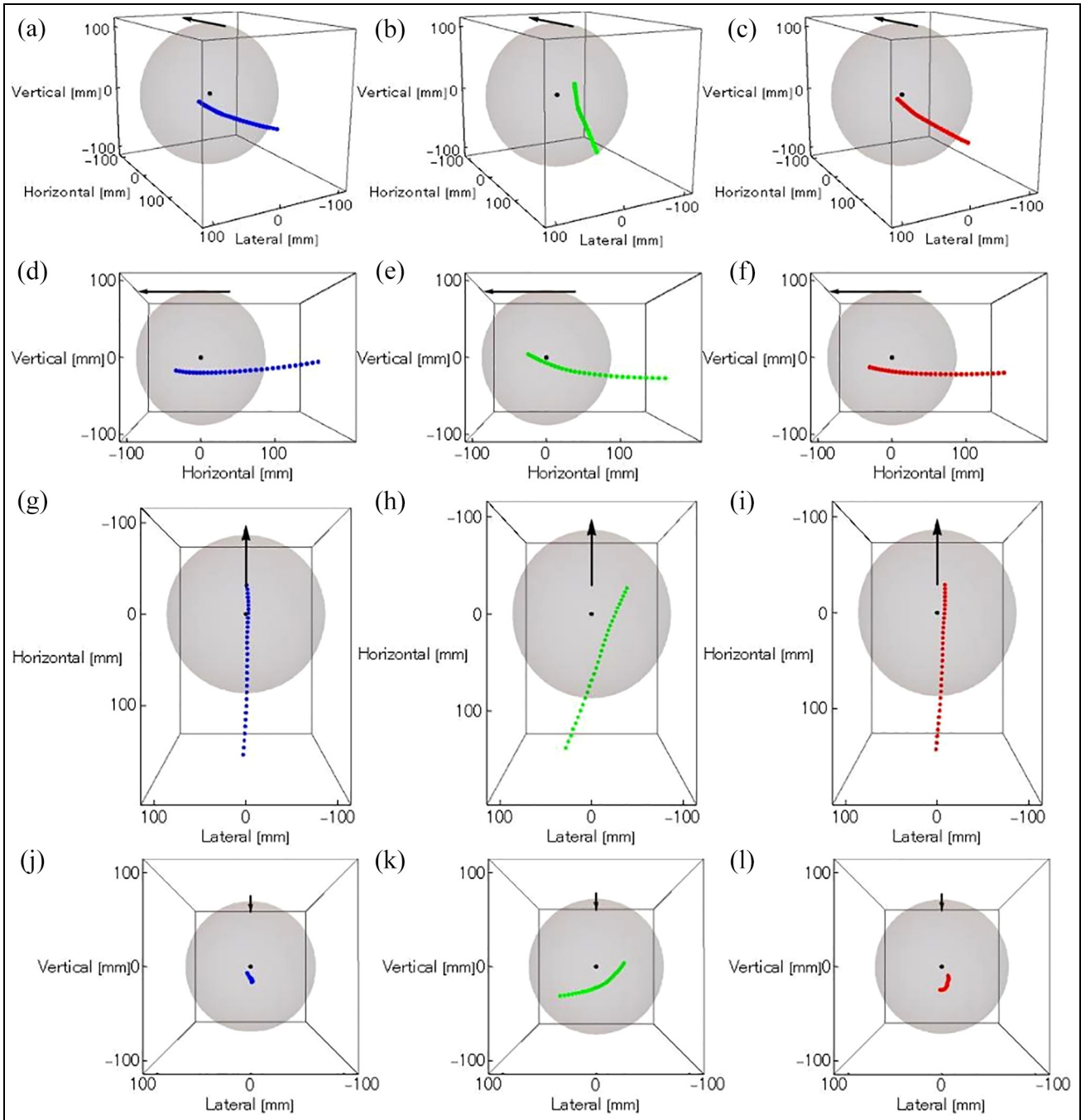


**Figure 7.** 3D perspectives of POF (impact point on foot) trajectories against the ball for the straight (a), curve (b), and knuckle (c) kicks; top views of the straight (d), curve (e) and knuckle (f) kicks; side views of the straight (g), curve (h), and knuckle (i) kicks; and rear views of the straight (j), curve (k), and knuckle (l) kicks. The arrow indicates the direction of ball movement in the trials.

analysis was 5.8 mm. This error risk is smaller than the differences of each component in the POF.

This study had several limitations. First, the form resolution of the virtual foot model in this study was relatively simple. Thus, the authors suggest that the model be further developed to better reflect the foot shape, thereby increasing the resolution of detection. The model applied in this study could detect impact

point differences as a first attempt. Second, the impact behaviour was analysed during the impact moment in this study; however, the ball deformation process was not considered. Deformations of the foot joint and ball or other interactions, such as stress distributions, need to be analysed and measured in future studies. Finally, the whole-body motion or joint torque that generated



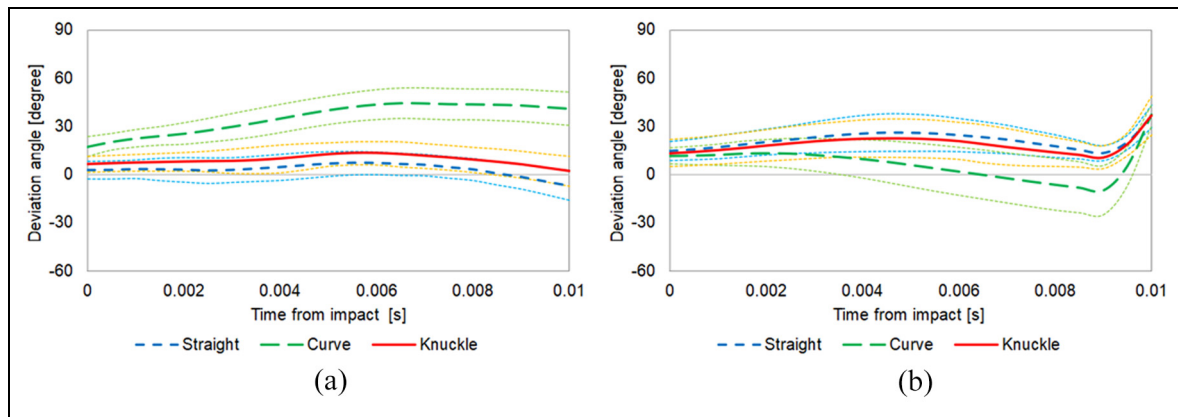


**Figure 8.** Transition of the mean swing vector deviation angle during ball impact in the horizontal plane (a) and sagittal plane (b) with each dashed standard deviation range.

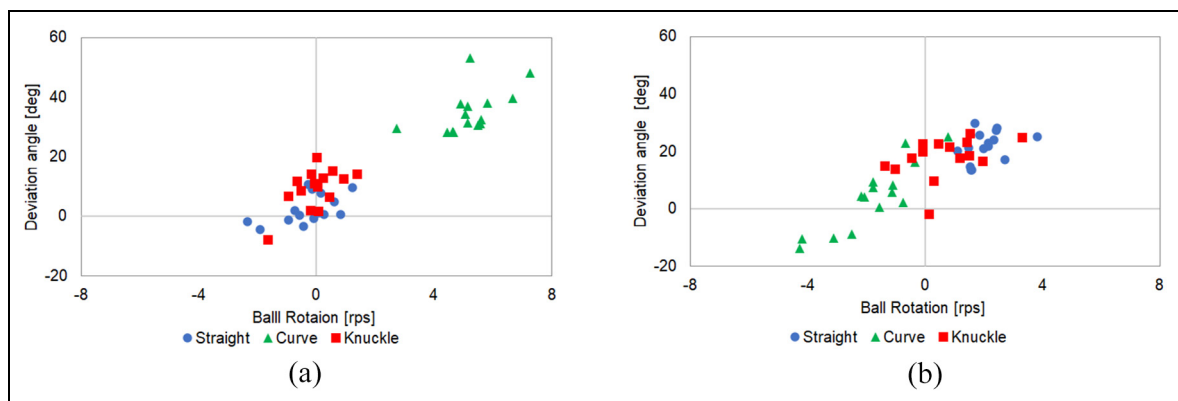


**Figure 9.** Correlation between the mean swing vector deviation angle and the ball rotation for all three types of kicks in the horizontal plane (a) and sagittal plane (b).

the analysed impact point behaviours was not clarified in this study and should be investigated in future research.

## Conclusion

The impact points of straight, curve, and knuckle kicks were obtained from observations of participant kicks. Capturing the three-dimensional location of the impact point and foot posture then allowed the face, swing vectors and attacking angle to be calculated in this study. The results indicate that the ball rotation was led by the swing vector calculated from the impact point trajectory relative to the centre of gravity of the ball.

The virtual modelling technique used to detect the impact points can reveal the relationship of impact phenomenon and ball behaviour when kicking. The use of this three-dimensional technique made the estimation of kicking motion more accurate than previous studies and useful for players to improve their skill. The virtual modelling technique can also be adapted to other sports involving kicking motions, such as rugby or

American football, as the ball surface model can easily be deformed to suit an elliptical sphere. Additional analysis considering the different objectives of kicking in different sports will be enabled by impact-point detection using virtual-modelling techniques.

## Authors' Note

Sungchan Hong is now affiliated to Institute for Liberal Arts, Tokyo Institute of Technology, Tokyo, Japan. Shuji Shimonagata is now affiliated to Faculty of Education, Chiba University, Chiba, Japan.

## Acknowledgements

The authors would like to thank Editage ([www.editage.com](http://www.editage.com)) for English language editing.


## Declaration of conflicting interests


The author(s) declared no potential conflicts of interest with respect to the research, authorship, and/or publication of this article.

## Funding

The author(s) received no financial support for the research, authorship, and/or publication of this article.

## ORCID iDs

Kaoru Kimachi  <https://orcid.org/0000-0001-7249-209X>

Sungchan Hong  <https://orcid.org/0000-0003-0149-5028>

## References

- Asami T. Analysis of powerful ball kicking. *Biomechanics VIII-B* 1983;695–700.
- Nunome H, Ikegami Y, Kozakai R, et al. Segmental dynamics of soccer instep kicking with the preferred and non-preferred leg. *J Sports Sci* 2006; 24(5): 529–541.
- Ishii H, Yanagiya T, Naito H, et al. Theoretical study of factors affecting ball velocity in instep soccer kicking. *J Appl Biomech* 2012; 28(3): 258–270.
- Peacock JCA and Ball K. The relationship between football impact and flight characteristics in punt kicking. *Sports Eng* 2017; 20(3): 221–230.
- Asai T, Carre MJ, Akatsuka T, et al. The curve kick of a football I: Impact with the foot. *Sports Eng* 2002; 5(4): 183–192.
- Asai T, Takano S, Carré MJ, et al. A fundamental study of an in front curve kick in football. *Proceedings*, 2004; 2: 183–192.
- Asai T, Seo K, Kobayashi O, et al. Fundamental aerodynamics of the soccer ball. *Sports Eng* 2007; 10(2): 101–109.
- Carre MJ, Asai T, Akatsuka T, et al. The curve kick of a football II: flight through the air. *Sports Eng* 2002; 5(4): 193–200.
- Bray K and Kerwin D. Modelling the flight of a soccer ball in a direct free kick. *J Sports Sci* 2003; 21(2): 75–85.
- Murakami M, Kondoh M, Iwai Y, et al. Measurement of aerodynamic forces and flow field of a soccer ball in a wind tunnel for knuckle effect. *Procedia Eng* 2010; 2(2): 2467–2472.
- Hong S, Chung C, Sakamoto K, et al. Analysis of the swing motion on knuckling shot in soccer. *Procedia Eng* 2011; 13:176–181.
- Hong S, Kazama Y, Nakayama M, et al. Ball impact dynamics of knuckling shot in soccer. *Procedia Eng* 2012; 34:200–205.
- Goff JE, Hobson CM, Asai T, et al. Wind-tunnel experiments and trajectory analyses for five nonspinning soccer balls. *Procedia Eng* 2016; 147(2016): 32–37.
- Asai T, Hong S, Kimachi K, et al. Flow visualisation around spinning and non-spinning soccer balls using the lattice Boltzmann method. *Proceedings* 2018; 2(6): 237.
- Asai T, Seo K, Kobayashi O, et al. Flow visualization on a real flight non-spinning and spinning soccer ball. In: Moritz EF and Haake S (eds) *The Engineering of Sport 6*. New York: Springer, 2006, pp.327–332.
- Asai T, Seo K, Sakurai Y, et al. A study of knuckling effect of soccer ball (P106). *Eng Sport* 2008; 1:555–562.
- Hong S, Chung C, Nakayama M, et al. Unsteady aerodynamic force on a knuckleball in soccer. *Procedia Eng* 2010; 2(2): 2455–2460.
- Lees A and Nolan L. The biomechanics of soccer: a review. *J Sports Sci* 1998; 16(3): 211–234.
- Lees A, Asai T, Andersen TB, et al. The biomechanics of kicking in soccer: a review. *J Sports Sci* 2010; 28(8): 805–817.
- Peacock J and Ball K. Is there a sweet spot on the foot in Australian football drop punt kicking? *J Sports Sci* 2019; 37(4): 467–476.
- Kimachi K, Hong S, Shimonagata S, et al. Impact points and their effect on Trajectory in soccer. *Proceedings* 2018; 2(6): 235.
- Kouchi M. Inter-generation differences in foot morphology: aging or secular change? *J Hum Ergol* 2003; 32(1): 23–48.
- Cohen J. *Statistical power analysis for the behavioral sciences*. New York, NY: Academic, 1988, pp.54.
- Rosenthal R. Parametric measures of effect size. In: Cooper H, Hedges LV and Valentine JC (eds) *The handbook of research synthesis*. New York: Russell SAGE Foundation, 1994, pp.231–244.
- Passmore MA, Tuplin S and Stawski A. The real-time measurement of football aerodynamic loads under spinning conditions. *Proc IMechE, Part P: J Sports Engineering and Technology* 2017; 231(4): 262–274.